

## Article

# Biochar/Clay Composite Particle Immobilized Compound Bacteria: Preparation, Collaborative Degradation Performance and Environmental Tolerance

Pengfei Sun <sup>1,2,3</sup>, Jun Wei <sup>4</sup>, Yaoyao Gao <sup>4</sup>, Zuhao Zhu <sup>1,2,3</sup> and Xiao Huang <sup>4,\*</sup>

<sup>1</sup> Ministry of Natural Resources, Fourth Institute of Oceanography, Beihai 536000, China; sunpengfei@4io.org.cn (P.S.); zhuzhao@4io.org.cn (Z.Z.)

<sup>2</sup> Key Laboratory of Tropical Marine Ecosystem and Bioresource, Ministry of Natural Resources, Beihai 536000, China

<sup>3</sup> Guangxi Beibu Gulf Key Laboratory of Marine Resources, Environment and Sustainable Development, Beihai 536000, China

<sup>4</sup> Jiangsu Key Laboratory of Atmospheric Environment Monitoring and Pollution Control, Collaborative Innovation Center of Atmospheric Environment and Equipment Technology, School of Environmental Science and Engineering, Nanjing University of Information Science and Technology, Nanjing 210000, China; 20211248087@nuist.edu.cn (J.W.); 202212480164@nuist.edu.cn (Y.G.)

\* Correspondence: 003199@nuist.edu.cn

**Abstract:** Immobilized microbial materials can effectively remove pollutants from surface water, and a biochar/clay composite particle (BCCP) material is prepared with immobilized *Flavobacterium mizutaii* sp. and *Aquamicrobium* sp. to remove ammonia nitrogen (NH<sub>4</sub><sup>+</sup>-N) and petroleum hydrocarbons (PHCs). The results indicated that the optimal ratios of biochar, Na<sub>2</sub>SiO<sub>3</sub> and NaHCO<sub>3</sub> were 15%, 3%, and 3%, and the adsorption process was found to be better described with the pseudo-second-order kinetic equation. The individual immobilization of *Flavobacterium mizutaii* sp. and *Aquamicrobium* sp. with sodium alginate–polyvinyl alcohol (PVA + SA) achieved 80% and 90% removal efficiencies for NH<sub>4</sub><sup>+</sup>-N and PHCs at the 10th d. The composite immobilization of two efficient bacteria could degrade 82.48% NH<sub>4</sub><sup>+</sup>-N and 74.62% PHCs. In addition, immobilization relieved the effects of temperature and salinity. This study can provide guidance for the application of immobilized microbial composite materials in natural water environments.

**Keywords:** biochar; composite particle; immobilization; compound bacteria; environmental tolerance



**Citation:** Sun, P.; Wei, J.; Gao, Y.; Zhu, Z.; Huang, X. Biochar/Clay Composite Particle Immobilized Compound Bacteria: Preparation, Collaborative Degradation Performance and Environmental Tolerance. *Water* **2023**, *15*, 2959. <https://doi.org/10.3390/w15162959>

Academic Editors: Xuan Ban, Wenxian Guo and Yicheng Fu

Received: 13 July 2023

Revised: 7 August 2023

Accepted: 14 August 2023

Published: 16 August 2023



**Copyright:** © 2023 by the authors. Licensee MDPI, Basel, Switzerland. This article is an open access article distributed under the terms and conditions of the Creative Commons Attribution (CC BY) license (<https://creativecommons.org/licenses/by/4.0/>).

## 1. Introduction

Wetland systems are special zones between marine and terrestrial ecosystems that play a crucial role in maintaining ecological balance [1]. The Liaohe Estuarine Wetland (LEW) is an important crab breeding area and also a reused oil extraction area. In recent years, aquaculture and oil exploration have led to excessive emissions of ammonia nitrogen (NH<sub>4</sub><sup>+</sup>-N) and severe petroleum pollution in wetland water systems, resulting in damage to the living environment of river crabs and affecting the ecological environment of wetlands [2]. Therefore, it is particularly important to control the concentrations of NH<sub>4</sub><sup>+</sup>-N and petroleum hydrocarbons (PHCs) in wetlands.

Secondary pollution during the removal of NH<sub>4</sub><sup>+</sup>-N and PHCs from surface water using conventional chemical methods used in wastewater treatment plants renders these methods unsuitable. The adsorption method has a wide application range and good treatment performance. Previous studies have shown that the use of biochar and clay to prepare biochar/clay composite particles (BCCP) to adsorb NH<sub>4</sub><sup>+</sup>-N has a significant effect [3]. However, adsorption alone cannot completely degrade petroleum pollutants such as PHCs. With the development of biotechnology, many microbial strains can be screened and applied for the degradation of NH<sub>4</sub><sup>+</sup>-N and PHCs. *Flavobacterium mizutaii*

sp. was reported as a predominant bacterial genus in the denitrification process and can effectively degrade  $\text{NH}_4^+\text{-N}$  in water [4]. *Aquamicrobium* sp. was found to be effective in degrading alkanes [5]. However, the use of high-efficiency bacterial agents is affected by the persistence of residence in freely flowing water bodies. Using BCCP as a carrier to immobilize efficient bacterial communities on BCCP can effectively maintain the concentration of microorganisms and provide pollutant degradation effects [6]. Meanwhile, environmental factors, such as salinity and temperature, restrict pollutant degradation, and it is necessary to study the degradation of pollutants by immobilized bacteria technology in wetlands [6]. The activity of nitrite oxidizing bacteria (NOB) gradually decreased as the salinity increased from approximately zero to 35.0 g/L [7]. When the temperature was lower than the optimal temperature, it affected the growth rate of bacteria, while higher temperatures reduced protein activity and even lead to cell death [8].

Sodium alginate (SA) and sodium alginate–polyvinyl alcohol (PVA + SA) as crosslinking materials can protect the bacteria against the intrusion of the environment [9]. Reddy and Osborne 2020 immobilized *Pseudomonas guariconensis* in the biocarrier matrix to degrade Reactive red 120, and the degradation efficiency could reach 91% [10]. Yan et al., 2020 found that the degradation efficiency of  $\text{Ca}^{2+}$  and  $\text{Mg}^{2+}$  can reach 90% and 70% under the action of immobilized *Lysinibacillus fusiformis* DB1-3 bacteria [11]. Hence, immobilization technology has good performance on the microbial degradation of pollutants. The previous research showed that the immobilized ammonia-oxidizing bacteria (AOB) could resist the influence of low temperature and maintained a good degradation efficiency [12]. However, LEW has received severe combined pollution of PHCs and  $\text{NH}_4^+\text{-N}$ , and whether immobilized composite microbial communities still have good effects is unknown. Hence, the degradation performance of combined immobilization of oil degrading bacteria and AOB needs further research.

In addition, the LEW is located in northern China and is affected by low temperature, high salinity and tides. The application of high-efficiency degrading bacteria is a challenge. Therefore, immobilization methods with BCCP do not only resist low temperature and high salinity but also avoid being dispersed by tides in the wetland. Immobilized BCCP is an effective method to solve the above problems, and its tolerance to low temperature and high salt needs to be further explored.

In this study, we investigated the effectiveness of immobilized microbial composite materials in removing  $\text{NH}_4^+\text{-N}$  and PHCs in wetland environments. (1) Orthogonal experiments and adsorption kinetics were studied to explore the optimal formulation of BCCP, and the adsorption effectiveness of BCCP on  $\text{NH}_4^+\text{-N}$  was investigated. (2) The degradation efficiency of  $\text{NH}_4^+\text{-N}$  and PHCs by BCCP immobilized with *Flavobacterium mizutaii* sp. and *Aquamicrobium* sp. was studied. (3) The tolerance to low temperatures and high salinity on the immobilized microorganisms was examined. This experiment can provide guidance for the application of immobilized microbial composite materials in wetlands.

## 2. Materials and Methods

### 2.1. Preparation of BCCP

Clay and reed stalk materials were obtained from the LEW. The reed stalks were repeatedly washed with deionized water to remove impurities. Then, they were placed in a crucible and dried at 105 °C for 24 h to eliminate any remaining moisture and impurities. The dried reed stalks were ground into powder using a mini plant grinder (FZ 102, Beijing Weiye, Nanhai, China), and the resulting powder was sieved to obtain particles with a size of 0.85 mm for further use. The reed stalk powder was subjected to carbonization in a pyrolyzer under a constant oxygen-limited condition with a heating rate of 10 °C per minute. The carbonization process was carried out at 600 °C for 3 h. Subsequently, the biochar and clay samples were crushed and sieved to obtain a uniform particle size of 0.15 mm. The biochar samples were dried at 105 °C for 24 h and then sealed in brown containers. Prior to use, they were rinsed multiple times with deionized water to remove any remaining

ash content. Detailed information regarding the characteristics of the biochar can be found in [3]. The specific preparation process of the biochar/clay is shown in Figure 1.

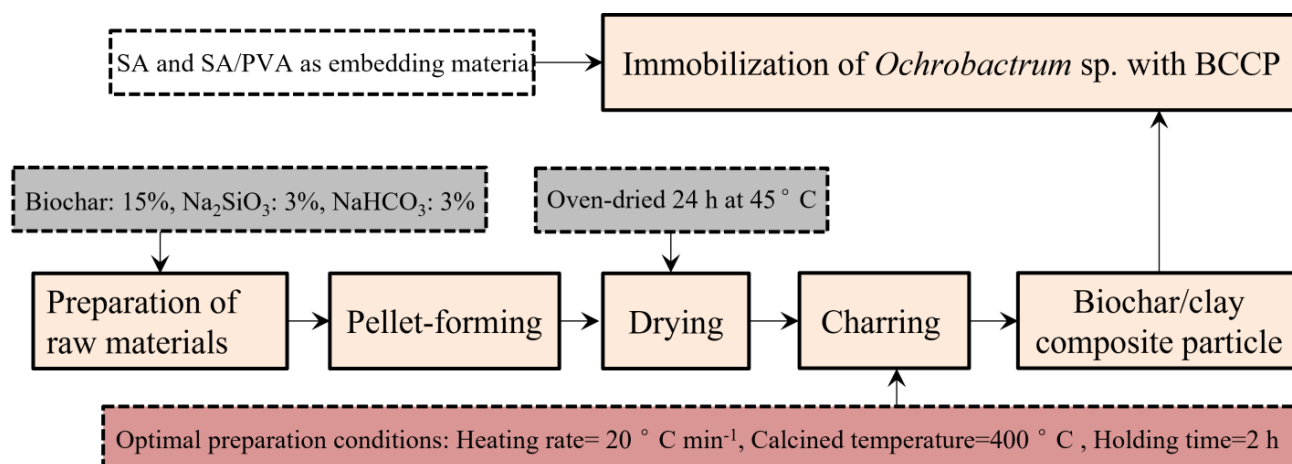


Figure 1. The preparation process of BCCP.

The formulation for the preparation of BCCP includes the base amount of binder, the amount of  $\text{Na}_2\text{SiO}_3$  and the amount of  $\text{NaHCO}_3$ . An orthogonal experiment,  $L_9 (3^4)$ , was conducted to optimize the best preparation method. The levels of the orthogonal experiment for the preparation formulation are shown in Table 1.

Table 1. The orthogonal test table level of BCCP preparation factors.

| Number. | Biochar Dosage (%) | $\text{Na}_2\text{SiO}_3$ Dosage (%) | $\text{NaHCO}_3$ Dosage (%) |
|---------|--------------------|--------------------------------------|-----------------------------|
| 1       | 5                  | 1                                    | 1                           |
| 2       | 5                  | 2                                    | 2                           |
| 3       | 5                  | 3                                    | 3                           |
| 4       | 10                 | 1                                    | 2                           |
| 5       | 10                 | 2                                    | 3                           |
| 6       | 10                 | 3                                    | 1                           |
| 7       | 15                 | 1                                    | 3                           |
| 8       | 15                 | 2                                    | 1                           |
| 9       | 15                 | 3                                    | 2                           |

## 2.2. *Flavobacterium mizutaii* sp. and *Aquamicrobium* sp.

The screening methods for *Flavobacterium mizutaii* sp. and *Aquamicrobium* sp. can be found in Huang et al., 2017 and Huang et al., 2022 [13,14]. The 16S rDNA gene of strain HXN-2 has been cloned and sequenced using the SeqMatch program in RDP (<http://rdp.cme.msu.edu/> (accessed on 10 July 2023)). In Figure 2, it has been classified that HXN-2 shows a 95% similarity to the 16S rDNA gene of *Aquamicrobium* sp. genus [13].

The 16S rDNA gene of strain SY-I has been cloned and sequenced, and the gene sequence has been submitted to GenBank. Using the SeqMatch program in RDP (<http://rdp.cme.msu.edu/> (accessed on 10 July 2023)) and conducting a BLAST analysis against the online database, it was found that SY-I shows a 94% similarity to the 16S rDNA gene of *Flavobacterium mizutaii* sp. Through searching for other closely related strains to SY-I and using software such as MNGA, a 16S rDNA phylogenetic tree has been constructed. Table 2 shows the physiological and chemical reactions of high-efficiency degrading bacteria.

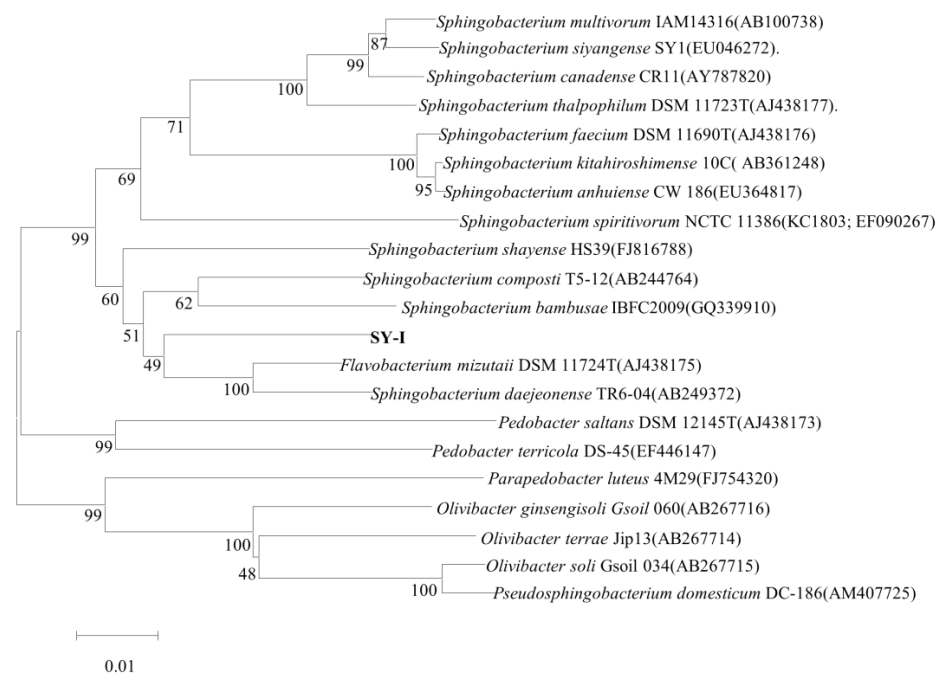


**Figure 2.** Phylogenetic tree of strain SY-I based on the complete sequences of the 16SrDNA gene.

**Table 2.** Physiological and biochemical responses of HXN-2 and SY-1.

| No. of Strains | Catalase Test | Starch Hydrolysis Test | Citrate Test | MR Test | Glucose Oxidation Fermentation Test | VP Test | Indole Test |
|----------------|---------------|------------------------|--------------|---------|-------------------------------------|---------|-------------|
| HXN-2          | +             | +                      | −            | +       | −                                   | −       | +           |
| SY-I           | −             | −                      | −            | +       | −                                   | +       | +           |

### 2.3. Adsorption kinetics of $\text{NH}_4^+\text{-N}$ by BCCP

In order to comprehensively understand the adsorption kinetics characteristics of biochar spheres on  $\text{NH}_4^+\text{-N}$ , this study used the pseudo-first-order kinetic Equation (1), pseudo-second-order kinetic Equation (2) and intra-particle diffusion model (3) to fit the experimental data.

$$q_t = q_e \left(1 - e^{-k_1 t}\right) \quad (1)$$

$$\frac{t}{q_t} = \frac{1}{k_2 q_e^2} + \frac{t}{q_e} \quad (2)$$

$$q_t = k_p \sqrt{t} + C \quad (3)$$

In the equations,  $k_1$  represents the rate constant of the pseudo-first-order kinetic equation,  $\text{min}^{-1}$ ;  $k_2$  represents the rate constant of the pseudo-second-order kinetic equation,  $\text{g/mg min}$ ;  $k_p$  represents the rate constant of intra-particle diffusion,  $\text{mg/g min}^{0.5}$ ;  $q_e$  represents the adsorption capacity of the biochar spheres, expressed in  $\text{mg/g}$ ; and  $q_t$  represents the adsorption capacity of the biochar spheres at time  $t$ ,  $\text{mg/g}$ .

### 2.4. Preparation of Immobilized Compound Bacteria

A 2% SA solution and a 12% PVA solution were prepared with deionized water. Then, a certain amount of  $\text{CaCl}_2$  was weighed and dissolved in deionized water to prepare a 2%  $\text{CaCl}_2$  solution. Both solutions dissolved in a constant-temperature water bath at  $100^\circ\text{C}$ , and the solution was then sterilized at  $121^\circ\text{C}$  and high pressure for 30 min. *Flavobacterium mizutaii* sp. and *Aquamicrobium* sp. were concentrated using a centrifuge at 4000 rpm,  $20^\circ\text{C}$  for 10 min once they were cultured in logarithmic growth phase ( $\text{OD}_{600} \approx 0.6$ ). The

supernatant was discarded and rinsed with sterile water to remove surface nutrients, and this process was repeated 2–3 times. The cultured and concentrated bacterial strains were mixed with the embedding material in a 1:2 ratio to obtain an embedding mixture. In addition, the BCCP was added into the embedding mixture and then removed into a 2% CaCl<sub>2</sub> solution, where gel particles formed. The prepared gel particles were placed in the sterilized CaCl<sub>2</sub> solution and then crosslinked in a refrigerator at 4 °C for 24 h.

### 2.5. Degradation of NH<sub>4</sub><sup>+</sup>-N and PHCs by Immobilized Compound Bacteria

The experiment involved the addition of four different treatments to a 100 mL solution containing NH<sub>4</sub><sup>+</sup>-N at a concentration of 50 mg L<sup>-1</sup> and PHCs at a concentration of 1000 mg L<sup>-1</sup>. The treatments included the following: (1) Control group: addition of BCCP alone; (2) FB group: addition of free bacteria; (3) P-B group: addition of BCCP followed by the adsorption of bacterial species; and (4) P-B-SA + PVA group: addition of BCCP with SA+PVA encapsulated bacterial species. The experiment was run continuously for 10 d to investigate the removal efficiency of NH<sub>4</sub><sup>+</sup>-N and PHCs. The concentration of NH<sub>4</sub><sup>+</sup>-N in the effluent was detected every day, and a sample of the effluent was taken every 3 days to test for PHCs.

### 2.6. Tolerances of Low Temperature and High Salinity

The preparation of high-efficiency bacteria with SA+PVA immobilized BCCP particles was based on the above immobilization method. They were placed separately under temperature conditions of 10, 15, 20, 25, 30 and 35 °C as well as salinity conditions of 10‰, 15‰, 20‰, 25‰, 30‰ and 35‰. They were run continuously to investigate the performance of temperature and salinity on NH<sub>4</sub><sup>+</sup>-N and PHCs degradation.

### 2.7. Analysis Methods

The determination method for NH<sub>4</sub><sup>+</sup>-N involves using Nessler's reagent and spectrophotometry. The analysis method for PHCs is as follows. Transfer the test water sample along with 2.0 g of anhydrous sulfuric acid to a 250 mL separating funnel and mix well. Add 10 mL of n-hexane and rinse the sample bottle twice with 10 mL of n-hexane; then, transfer all the rinsing solution to the separating funnel. Shake the separating funnel for 5 min (release any trapped gas), and let it stand for 10 min. After sufficient phase separation between the extract and the water sample, transfer the lower aqueous layer back to the original water sample bottle. Use filter paper to remove any moisture from the neck of the separating funnel. Transfer the n-hexane extract to a 50 mL stoppered colorimetric tube. Repeat the process two more times to ensure complete extraction of PHCs from the test sample. Transfer the extract to a 1 cm quartz cuvette and measure the absorbance (A) at a wavelength of 225 nm using n-hexane as a reference. Record the measured data and calculate the concentration of PHCs in the water sample according to Formula (4):

$$C_{oil} = \frac{QV_1}{V_2} \quad (4)$$

In the formula,  $C_{oil}$  represents the concentration of oil in the water sample, mg L<sup>-1</sup>;  $Q$  represents the concentration of oil in the n-hexane extract obtained from the standard curve, mg L<sup>-1</sup>;  $V_1$  represents the volume of n-hexane extraction solvent, mL; and  $V_2$  represents the volume of the sample, mL.

## 3. Results

### 3.1. Preparation and Condition Optimization of BCCP

#### 3.1.1. Effect of Preparation Formula on the Adsorption Characteristics of NH<sub>4</sub><sup>+</sup>-N

The control of the preparation formula (biochar dosage, Na<sub>2</sub>SiO<sub>3</sub> dosage and NaHCO<sub>3</sub> dosage) could change the surface structure of biochar to a certain extent and affect its adsorption performance for NH<sub>4</sub><sup>+</sup>-N [15]. Therefore, in this study, the orthogonal experiment

method was used to investigate the effect of the BCCP preparation formula on  $\text{NH}_4^+-\text{N}$  adsorption (Table 3). The preparation formula of BCCP had a great influence on the adsorption of  $\text{NH}_4^+-\text{N}$ . The minimum adsorption capacity was 0.452 mg/g; the maximum was 0.538 mg/g. With the dosage increase of the biochar,  $\text{Na}_2\text{SiO}_3$  and  $\text{NaHCO}_3$ , the adsorption capacity of the prepared biochar spheres showed an increasing trend. When the dosage ratio of biochar,  $\text{Na}_2\text{SiO}_3$  and  $\text{NaHCO}_3$  was 15%, 3% and 3%, the adsorption capacity of the biochar spheres was the largest, which was 0.528, 0.500 and 0.506 mg/g, respectively. This may be because the increase in biochar dosage increases the specific surface area of the biochar spheres and the porosity of the biochar spheres, which increases the adsorption capacity of the biochar spheres. The addition of the  $\text{Na}_2\text{SiO}_3$  crosslinking agent increased the interlayer distance of the clay on the basis of maintaining the original layered structure of the clay. Meanwhile, the addition of  $\text{Na}_2\text{SiO}_3$  increased the amount of  $\text{Na}_2\text{SiO}_3$  to generate  $\text{NaHCO}_3$  with  $\text{CO}_2$  in the air [3]. After the decomposition of  $\text{Na}_2\text{CO}_3$  at high temperature,  $\text{CO}_2$  was released, which promoted the formation of a microporous structure of the biochar spheres, thereby increasing the adsorption capacity of the biochar spheres [16].  $\text{NaHCO}_3$  is decomposed into  $\text{CO}_2$  at high temperature, which further increases the porosity of the material and enhances the adsorption capacity of  $\text{NH}_4^+-\text{N}$ .

**Table 3.** Orthogonal experiment results with different preparation formulas.

| Levels          | Biochar Dosage (%) | $\text{Na}_2\text{SiO}_3$ Dosage (%) | $\text{NaHCO}_3$ Dosage (%) | Result                     |
|-----------------|--------------------|--------------------------------------|-----------------------------|----------------------------|
|                 | A                  | B                                    | C                           | Adsorption Capacity (mg/g) |
| 1               | 5                  | 1                                    | 1                           | 0.452                      |
| 2               | 5                  | 2                                    | 2                           | 0.463                      |
| 3               | 5                  | 3                                    | 3                           | 0.484                      |
| 4               | 10                 | 1                                    | 2                           | 0.487                      |
| 5               | 10                 | 2                                    | 3                           | 0.495                      |
| 6               | 10                 | 3                                    | 1                           | 0.491                      |
| 7               | 15                 | 1                                    | 3                           | 0.538                      |
| 8               | 15                 | 2                                    | 1                           | 0.521                      |
| 9               | 15                 | 3                                    | 2                           | 0.526                      |
| Average value 1 | 0.466              | 0.492                                | 0.488                       |                            |
| Average value 2 | 0.491              | 0.493                                | 0.492                       | 0.506                      |
| Average value 3 | 0.528              | 0.500                                | 0.506                       |                            |

Table 4 shows the range analysis of  $\text{NH}_4^+-\text{N}$  adsorption by BCCP preparation formula, and the primary and secondary relationships of the influence of three factors on  $\text{NH}_4^+-\text{N}$  adsorption were judged by the range. Through the experimental results  $T_3 > T_1 > T_2$ , it showed that the primary and secondary relationships affecting the adsorption capacity of the biochar spheres were CAB ( $\text{NaHCO}_3$  dosage > biochar dosage >  $\text{Na}_2\text{SiO}_3$  dosage). Through the analysis of the influence of each factor, it was concluded that  $\text{A}_3\text{B}_3\text{C}_3$  was the best biochar configuration formula, and the corresponding parameters were biochar 15%,  $\text{Na}_2\text{SiO}_3$  3% and  $\text{NaHCO}_3$  3%.

**Table 4.** The range analysis of  $\text{NH}_4^+-\text{N}$  adsorption with different biochar preparation formulas.

| Levels           | Factor                                       |                        |                        |  |       |
|------------------|--|------------------------|------------------------|--|-------|
|                  | $\delta_1$                                   | $\delta_2$             | $\delta_3$             | R                                      | T     |
| 1                | $\delta_{11} = -0.029$                       | $\delta_{21} = -0.003$ | $\delta_{31} = -0.007$ | $R_{01} = -0.003$<br>$R_{11} = -0.029$ | 0.026 |
| 2                | $\delta_{12} = -0.004$                       | $\delta_{22} = -0.002$ | $\delta_{32} = -0.003$ | $R_{02} = -0.002$<br>$R_{12} = -0.004$ | 0.002 |
| 3                | $\delta_{13} = 0.033$                        | $\delta_{23} = 0.005$  | $\delta_{33} = 0.011$  | $R_{03} = 0.033$<br>$R_{13} = 0.005$   | 0.028 |
| Primary relation | CAB  |                        |                        |  |       |
| Optimal scheme   | $\text{A}_3\text{B}_3\text{C}_3$ (15%–3%–3%) |                        |                        |  |       |



### 3.1.2. Effect of Raw Material Ratio on $\text{NH}_4^+$ -N Adsorption

By fitting the experimental data of different biochar dosages and different  $\text{NaHCO}_3$  dosages, the quasi-first-order kinetic equation, quasi-second-order kinetic equation and intra-particle diffusion model of  $\text{NH}_4^+$ -N adsorption by the biochar spheres were obtained. The kinetic model parameters and correlation coefficients are shown in Tables 5 and 6, respectively. By comparing the correlation coefficients, the quasi-second-order kinetic equation is more suitable for the adsorption of  $\text{NH}_4^+$ -N by BCCP than the quasi-first-order kinetic equation and the intra-particle diffusion equation under the conditions of different biochar dosages and different  $\text{NaHCO}_3$  dosages. Intra-particle diffusion is not the control step to control the adsorption rate.

**Table 5.** The adsorption kinetic parameters of BCCP with different biochar dosing quantities.

| Biochar<br>Clay | Pseudo-First-Order |                                   |                    |       | Pseudo-Second-Order |                    |       | Intra-Particle Diffusion            |       |
|-----------------|--------------------|-----------------------------------|--------------------|-------|---------------------|--------------------|-------|-------------------------------------|-------|
|                 | $q_e$<br>(mg/g)    | $K^{-1}$<br>( $\text{min}^{-1}$ ) | $q_{eq}$<br>(mg/g) | $R^2$ | $K_2$<br>(g/mg min) | $q_{eq}$<br>(mg/g) | $R^2$ | $k_p$<br>(g/mg $\text{min}^{0.5}$ ) | $R^2$ |
| 5%              | 0.450              | 0.036                             | 0.455              | 0.929 | 0.093               | 0.513              | 0.986 | 0.024                               | 0.944 |
| 10%             | 0.482              | 0.036                             | 0.469              | 0.939 | 0.088               | 0.530              | 0.991 | 0.025                               | 0.944 |
| 15%             | 0.518              | 0.039                             | 0.495              | 0.916 | 0.092               | 0.557              | 0.983 | 0.026                               | 0.945 |

**Table 6.** The adsorption kinetic parameters of BCCP with different  $\text{NaHCO}_3$  dosing quantities.

| $\text{Na}_2\text{CO}_3$<br>Clay | Pseudo-First-Order |                                   |                    |       | Pseudo-Second-Order |                    |       | Intra-Particle Diffusion            |       |
|----------------------------------|--------------------|-----------------------------------|--------------------|-------|---------------------|--------------------|-------|-------------------------------------|-------|
|                                  | $q_e$<br>(mg/g)    | $K^{-1}$<br>( $\text{min}^{-1}$ ) | $q_{eq}$<br>(mg/g) | $R^2$ | $K_2$<br>(g/mg min) | $q_{eq}$<br>(mg/g) | $R^2$ | $k_p$<br>(g/mg $\text{min}^{0.5}$ ) | $R^2$ |
| 1.0%                             | 0.395              | 0.035                             | 0.370              | 0.877 | 0.117               | 0.414              | 0.959 | 0.019                               | 0.960 |
| 2.0%                             | 0.404              | 0.029                             | 0.385              | 0.899 | 0.091               | 0.435              | 0.953 | 0.021                               | 0.961 |
| 3.0%                             | 0.411              | 0.039                             | 0.394              | 0.934 | 0.121               | 0.440              | 0.985 | 0.020                               | 0.928 |

The pseudo-second-order kinetic equation can better describe the adsorption process of  $\text{NH}_4^+$ -N by the biochar spheres [17]. The model includes all the processes of biochar sphere adsorption, namely external membrane diffusion, surface adsorption and intraparticle diffusion. Compared with the pseudo-first-order kinetic model, the formation of chemical bonds affects the pseudo-second-order kinetic adsorption and is the main reason [18], indicating that the adsorption process of BCCP on  $\text{NH}_4^+$ -N is mainly chemical adsorption.

The adsorption process of BCCP can be divided into three stages, namely external diffusion, internal diffusion (pore internal diffusion) and adsorption reaction stage, and finally, the adsorption equilibrium is reached [19]. In the internal diffusion model, it indicates that the internal diffusion is the rate-determining step of the reaction during the adsorption process. However, the internal diffusion fitting curve did not pass the coordinate origin in this study, which indicated that the internal diffusion was not the only rate-determining step in the adsorption process of  $\text{NH}_4^+$ -N by BCCP.

### 3.2. Performances of Individual AOB and Petroleum-Degrading Bacteria Immobilization

As a carrier for microbial immobilization, BCCP can avoid the dispersion of free bacteria and reduce its pollutant degradation performance, which is a common and effective method [20]. However, whether immobilization becomes the main controlling factor limiting the conversion of pollutants needs further research. In this study, the individual immobilization of AOB and petroleum-degrading bacteria were studied to discuss the degradation efficiency of  $\text{NH}_4^+$ -N and PHCs, and the results are shown in Figure 3A,B.

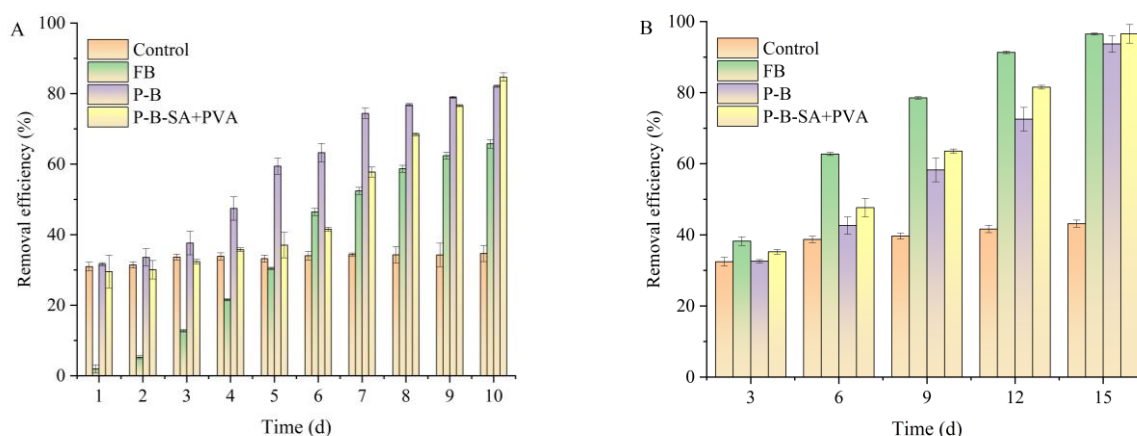


**Figure 3.** Effect of BCCP-immobilized AOB (A) and petroleum-degrading bacteria (B).

### 3.2.1. NH<sub>4</sub><sup>+</sup>-N Removal Performance with Immobilized *Flavobacterium mizutaii* sp.

Figure 3A demonstrates the degradation performance of BCCP-immobilized AOB on NH<sub>4</sub><sup>+</sup>-N. The removal efficiency of NH<sub>4</sub><sup>+</sup>-N in the control group (only added BCCP) was stable at approximately 30%. The control group did not add bacteria but had a certain adsorption effect, which relied on the adsorption of the BCCP themselves. In the experimental group of (FB) (only free bacteria and no composite particles), the effect was little in the first 2 d, and the degradation efficiency was less than 10%. Then, with the time extending, the degradation efficiency continued to increase and reached 65.74% at 10 d.

The experimental groups of P-B (BCCP adsorbed the bacteria) and the SA + PVA combined embedding bacteria increased with the time extending and reached more than 80% at 10 d. The NH<sub>4</sub><sup>+</sup>-N rapid adsorption performance of the P-B and P-B-SA + PVA groups at the beginning resulted in a higher removal performance than free bacteria. However, the effect of the P-B-SA + PVA group is lower than that of the P-B group after a period of time, and then the removal efficiency of the P-B-SA + PVA group restored and equivalented to the P-B group with the further extension of the reaction time. It indicated that the embedding first had a certain inhibitory effect on the experiment, and then the permeability became stronger, and the degradation effect was significantly improved with the increase in enrichment [6]. The results showed that BCCP could improve the degradation efficiency of NH<sub>4</sub><sup>+</sup>-N as the carrier of immobilized AOB. Due to the porous structure of the biochar sphere that provides a larger surface area and more pores, it can store more substrates and promote the growth of microorganisms [21].

### 3.2.2. The Effect of Immobilized *Aquamicrobium* sp. on the Removal of PHCs

Figure 3B shows the removal efficiency of PHCs under different conditions. From the figure, it can be observed that the PHC degradation in the control group with the addition of BCCP exhibited a gradual increase from 32.45% on the 3rd d to 43.14% on the 15th d, which indicated the process was only adsorption efficiency. However, upon the addition of bacterial strains, the removal efficiency of PHCs significantly improved. FB, P-B and P-B-SA + PVA demonstrated removal efficiencies of 96.48%, 93.69% and 96.53% for PHCs at the 15th d, respectively. Notably, P-B-SA + PVA showed superior removal performance compared to PB, primarily due to its porous structure, which enhances PHC adsorption while providing a larger substrate reservoir to promote microbial growth [22].

### 3.3. Performance of Immobilized Compound Bacteria

Individual immobilization of *Aquamicrobium* sp. and *Flavobacterium mizutaii* sp. showed better degradation effects for NH<sub>4</sub><sup>+</sup>-N and PHCs. However, whether the composite embedding of the two bacterial communities still has the same effect for NH<sub>4</sub><sup>+</sup>-N and PHCs removal needs to be studied and is demonstrated in Figure 4. At the 1st d, the degradation effects of NH<sub>4</sub><sup>+</sup>-N and PHCs by the two bacteria were unsatisfactory at only 28.74% and



32.5%, respectively. With the time extending, the adaptability of the flora to the environment was enhanced, and the abundance of microorganisms was enriched [23], resulting in increased degradation of  $\text{NH}_4^+\text{-N}$  and PHCs. At the 10th d, the degradation efficiency reached 74.62% and 82.48%, respectively. Compared with the individual immobilized *Aquamicrobium* sp. and *Flavobacterium mizutaii* sp. (the removal efficiencies of  $\text{NH}_4^+\text{-N}$  and PHCs were 84.69% and 96.53%), the removal efficiencies of  $\text{NH}_4^+\text{-N}$  and PHCs with the immobilized compound bacteria were slightly reduced (individual immobilized bacteria was 10.07% and 14.05% higher than those by the composite embedding).

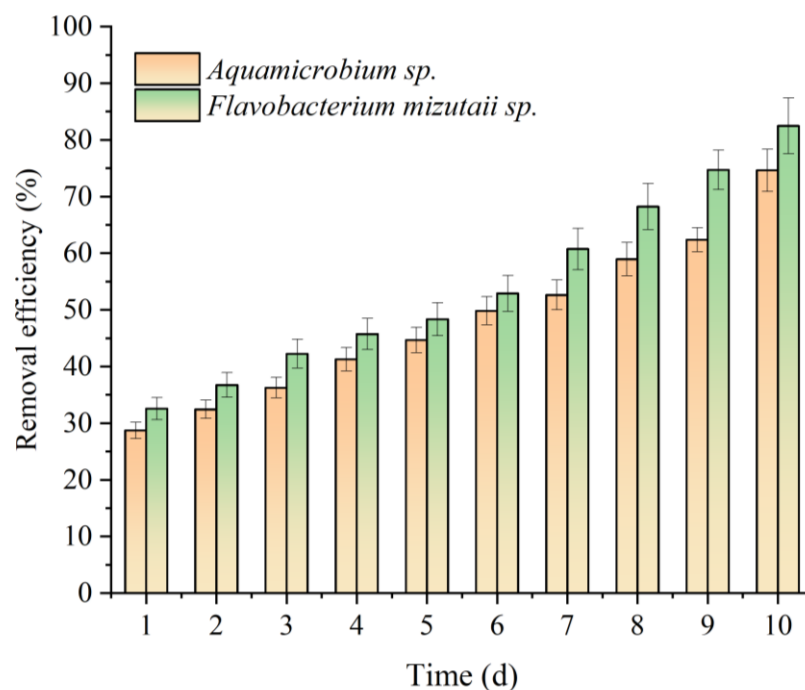


**Figure 4.** Removal performance of immobilized compound bacteria on  $\text{NH}_4^+\text{-N}$  and PHCs.

### 3.4. Tolerance of Immobilized Compound Bacteria to Low Temperature and High Salinity

#### 3.4.1. Tolerance to Temperature

Temperature is an important environmental factor that affects microbial growth. Figure 5A demonstrates the effect of temperature on the degradation of  $\text{NH}_4^+\text{-N}$  and PHCs by immobilized *Flavobacterium mizutaii* sp. and *Aquamicrobium* sp. As the temperature gradually increased, the degradation efficiency of  $\text{NH}_4^+\text{-N}$  and PHCs also increased. At 10 °C, the removal efficiencies of  $\text{NH}_4^+\text{-N}$  and PHCs were 52.5% and 41.25%, respectively. However, as the temperature rose to 35 °C, the removal efficiencies of  $\text{NH}_4^+\text{-N}$  and PHCs increased to 92.76% and 89.92%, respectively. When the temperature was lower than the optimal growth temperature for *Flavobacterium mizutaii* sp. and *Aquamicrobium* sp., the intracellular activity within the microbial cells decreased, which led to a slower growth rate of bacteria [24]. The previous study by Huang et al. (2017) confirmed that the *Aquamicrobium* sp. was a cold-tolerant AOB and could degrade 53.48%  $\text{NH}_4^+\text{-N}$  when the temperature was 15 °C [13]. The high removal efficiency reflected by SA and PVA immobilization with BCCP is owed to cold-resistant function. Meanwhile, Huang et al. (2022) utilized SA and PVA immobilized petroleum degrading bacteria and found it to have certain salt- and cold-resistance performances [14].

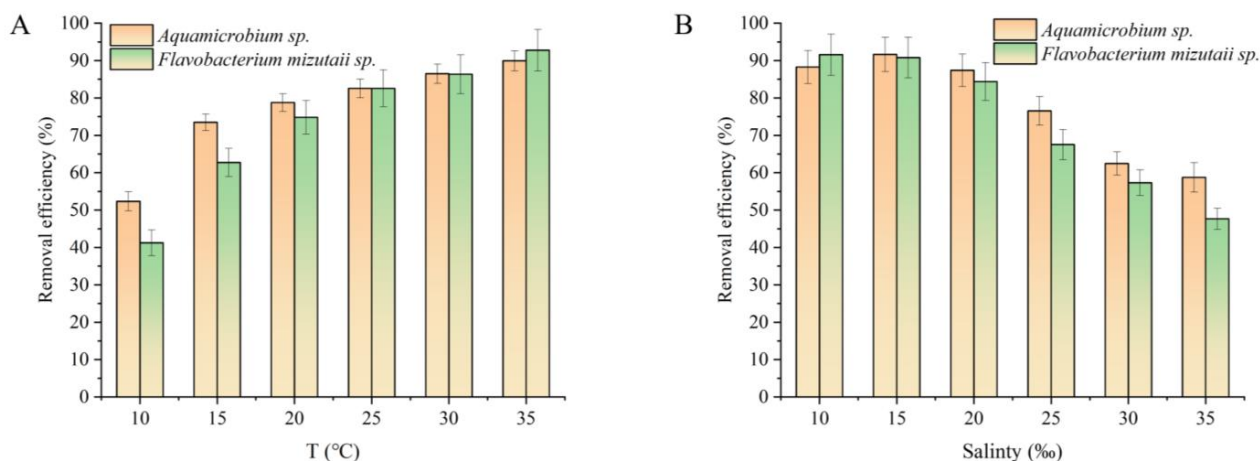


**Figure 5.** Effects of temperature (A) and salinity (B) on immobilized compound bacteria.

### 3.4.2. Tolerance to Salinity

Salinity is another important environmental factor that affects microbial growth. As shown in Figure 5B, the optimal salinity for the degradation of  $\text{NH}_4^+\text{-N}$  and PHCs is 15‰ with removal efficiencies of 88.27% and 91.64%, respectively. However, as salinity increases, the removal efficiencies of PHCs and  $\text{NH}_4^+\text{-N}$  continuously decrease. At a salinity of 35‰, the removal efficiencies of  $\text{NH}_4^+\text{-N}$  and PHCs decrease to 58.74% and 47.68%, respectively. This is mainly due to the impact of high salt environments on cell osmotic pressure, leading to a decrease in microbial abundance [25]. Gao et al., 2020 found that immobilization materials provide protection to bacteria in high-salinity environments [25]. When salinity exceeds 15‰, bacterial growth is inhibited, which is consistent with the findings of this study. The previous study by Huang et al., 2017 found that the *Aquamicrobium sp.* was a salt-tolerant AOB, and the  $\text{NH}_4^+\text{-N}$  removal efficiency could reach 60% when the salinity was 20‰ [13]. In this study, the removal efficiencies were 58.74% and 47.68% under the conditions of 35‰ and 20‰, which indicated the SA and PVA immobilization with BCCP can protect bacteria and slow down the impact of high salinity.

### 3.5. $\text{NH}_4^+\text{-N}$ and PHCs Degradation Mechanism with BCCP Immobilization

Based on the above research, a preliminary discussion of the mechanisms underlying the degradation of  $\text{NH}_4^+\text{-N}$  by immobilized *Flavobacterium mizutaii sp.* and the degradation of PHCs by *Aquamicrobium sp.* has been conducted and is illustrated in Figure 6. The BCCP exhibits physical adsorption, which facilitates the rapid adsorption and accumulation of  $\text{NH}_4^+\text{-N}$  and PHCs, providing better conditions for subsequent microbial degradation. Additionally, the encapsulation of bacterial populations within the biochar spheres allows for the degradation of high concentrations of  $\text{NH}_4^+\text{-N}$ . The porous nature of biochar provides a habitat for the bacterial community, and its adsorption capacity promotes microbial transformation, leading to the degradation of  $\text{NH}_4^+\text{-N}$  and PHCs [26]. In summary, the BCCP contribute to the effective removal of  $\text{NH}_4^+\text{-N}$  and PHCs through physical adsorption, while the encapsulation of bacterial populations within the biochar spheres and the porous nature of biochar provide favorable conditions for bacterial degradation and transformation processes, ultimately leading to the degradation of  $\text{NH}_4^+\text{-N}$  and PHCs.

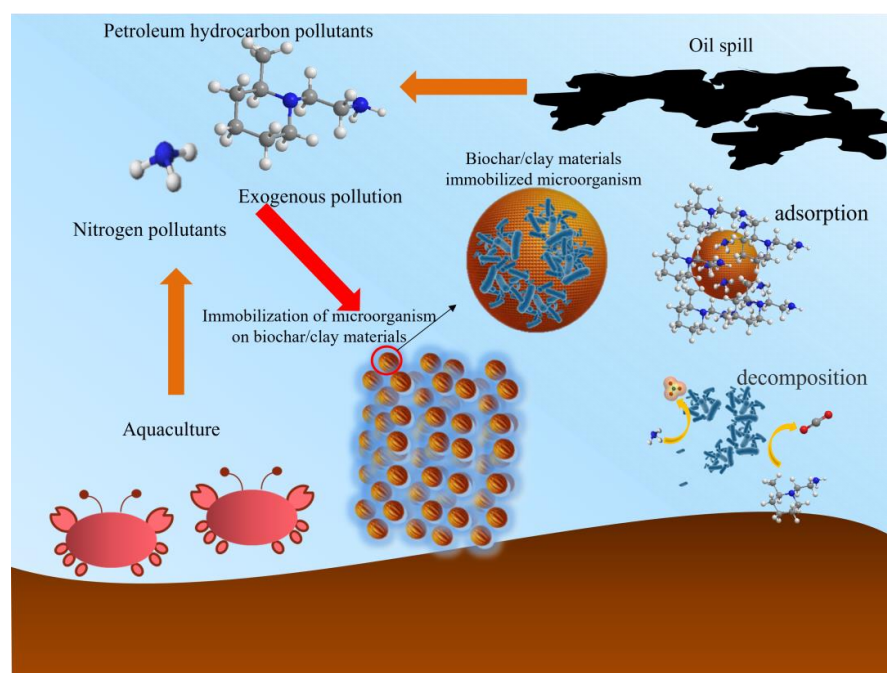


**Figure 6.**  $\text{NH}_4^+\text{-N}$  and PHCs removal mechanism by immobilization of compound bacteria on BCCP.

#### 4. Conclusions

The results showed that the optimal composition of BCCP was 15% biochar, 3%  $\text{Na}_2\text{SiO}_3$  and 3%  $\text{NaHCO}_3$ . The primary and secondary factors influencing the adsorption capacity were  $\text{NaHCO}_3$  dosage > biochar dosage >  $\text{Na}_2\text{SiO}_3$  dosage. The adsorption process of BCCP for  $\text{NH}_4^+\text{-N}$  fitted the pseudo-second-order kinetic equation. Individual immobilization of AOB (*Flavobacterium mizutaii* sp.) and petroleum-degrading bacteria (*Aquamicrobium* sp.) owned higher removal efficiencies (84.69% and 96.53%) than free bacteria. Compared with the individual immobilized *Aquamicrobium* sp. and *Flavobacterium mizutaii* sp., the removal efficiencies of  $\text{NH}_4^+\text{-N}$  and PHCs with immobilizing compound bacteria were reduced by 10.07% and 14.05%. In addition, immobilization relieved the effects of low temperature and high salinity.

**Author Contributions:** P.S.: Data curation, Visualization, Methodology, Formal analysis, Writing—original draft. J.W.: Conceptualization, Supervision, Validation, Writing—review and editing. Y.G.: Conceptualization, Formal analysis, Writing—review and editing. Z.Z.: Writing—review and editing. X.H.: Funding acquisition, Writing—review and editing. All authors have read and agreed to the published version of the manuscript.

**Funding:** This study was funded by the National Natural Science Foundation of China (No. U20A20103), the Special Project of Guangxi Science and Technology Base and Talent (No. GUIKE AD20297065), the Scientific Research Fund of the Fourth Institute of Oceanography (No. 202003), the Science and Technology Planning Projects of Beihai, Guang xi, China (No. 202082042 and 202082031) and the National Major Project of Water Pollution Control and Management Technology in China (No. 2013ZX07202-007).

**Data Availability Statement:** The data that support the findings of this study are available on request from the corresponding author H. X. upon reasonable request.

**Conflicts of Interest:** The authors declare no conflict of interest.

#### References

- Saha, T.K.; Pal, S. Exploring physical wetland vulnerability of Atravee river basin in India and Bangladesh using logistic regression and fuzzy logic approaches. *Ecol. Indic.* **2018**, *98*, 251–265. [CrossRef]
- Duan, M.; Li, C.; Wang, X.; Fang, S.; Xiong, Y.; Shi, P. Solid separation from the heavy oil sludge produced from Liaohe Oilfield. *J. Pet. Sci. Eng.* **2018**, *172*, 1112–1119. [CrossRef]

3. Huang, X.; Bai, J.; Li, K.; Zhao, Y.; Tian, W.; Hu, C. Preparation of Clay/Biochar Composite Adsorption Particle and Performance for Ammonia Nitrogen Removal from Aqueous Solution. *J. Ocean Univ. China* **2020**, *19*, 729–739. [[CrossRef](#)]
4. Chen, Y.; Wang, X.; Wang, X.; Cheng, T.; Fu, K.; Qin, Z.; Feng, K. Biofilm Structural and Functional Features on Microplastic Surfaces in Greenhouse Agricultural Soil. *Sustainability* **2022**, *14*, 7024. [[CrossRef](#)]
5. Shahi, A.; Aydin, S.; Ince, B.; Ince, O. Evaluation of microbial population and functional genes during the bioremediation of petroleum-contaminated soil as an effective monitoring approach. *Ecotoxicol. Environ. Saf.* **2016**, *125*, 153–160. [[CrossRef](#)] [[PubMed](#)]
6. Sun, P.; Huang, X.; Xing, Y.; Dong, W.; Yu, J.; Bai, J.; Duan, W. Immobilization of *Ochrobactrum* sp. on Biochar/Clay Composite Particle: Optimization of Preparation and Performance for Nitrogen Removal. *Front. Microbiol.* **2022**, *13*, 838836. [[CrossRef](#)]
7. He, H.; Chen, Y.; Li, X.; Cheng, Y.; Yang, C.; Zeng, G. Influence of salinity on microorganisms in activated sludge processes: A review. *Int. Biodeterior. Biodegradation* **2016**, *119*, 520–527. [[CrossRef](#)]
8. Nwoba, E.G.; Parlevliet, D.A.; Laird, D.W.; Alameh, K.; Moheimani, N.R. Light management technologies for increasing algal photobioreactor efficiency. *Algal Res.* **2019**, *39*, 101433. [[CrossRef](#)]
9. Angelim, A.L.; Costa, S.P.; Farias, B.C.S.; Aquino, L.F.; Melo, V.M.M. An innovative bioremediation strategy using a bacterial consortium entrapped in chitosan beads. *J. Environ. Manag.* **2013**, *127*, 10–17. [[CrossRef](#)]
10. Reddy, S.; Osborne, J.W. Biodegradation and biosorption of Reactive Red 120 dye by immobilized *Pseudomonas guariconensis*: Kinetic and toxicity study. *Water Environ. Res.* **2020**, *92*, 1230–1241. [[CrossRef](#)]
11. Yan, H.; Han, Z.; Zhao, H.; Pan, J.; Zhao, Y.; Tucker, M.E.; Zhou, J.; Yan, X.; Yang, H.; Fan, D. The bio-precipitation of calcium and magnesium ions by free and immobilized *Lysinibacillus fusiformis* DB1-3 in the wastewater. *J. Clean. Prod.* **2019**, *252*, 119826. [[CrossRef](#)]
12. Huang, X.; Bai, J.; Li, K.-R.; Zhao, Y.-G.; Tian, W.-J.; Dang, J.-J. Characteristics of two novel cold- and salt-tolerant ammonia-oxidizing bacteria from Liaohe Estuarine Wetland. *Mar. Pollut. Bull.* **2017**, *114*, 192–200. [[CrossRef](#)]
13. Huang, X.; Zhou, T.; Chen, X.; Bai, J.; Zhao, Y. Enhanced Biodegradation of High-Salinity and Low-Temperature Crude-Oil Wastewater by Immobilized Crude-Oil Biodegrading Microbiota. *J. Ocean Univ. China* **2022**, *21*, 141–151. [[CrossRef](#)]
14. Mahdi, Z.; Yu, Q.J.; El Hanandeh, A. Removal of lead(II) from aqueous solution using date seed-derived biochar: Batch and column studies. *Appl. Water Sci.* **2018**, *8*, 181. [[CrossRef](#)]
15. Ojeda-López, R.; Ramos-Sánchez, G.; García-Mendoza, C.; Azevedo, D.C.S.; Guzmán-Vargas, A.; Felipe, C. Effect of Calcination Temperature and Chemical Composition of PAN-Derived Carbon Microfibers on N<sub>2</sub>, CO<sub>2</sub>, and CH<sub>4</sub> Adsorption. *Materials* **2021**, *14*, 3914. [[CrossRef](#)] [[PubMed](#)]
16. Xue, S.; Zhang, X.; Ngo, H.H.; Guo, W.; Wen, H.; Li, C.; Zhang, Y.; Ma, C. Food waste based biochars for ammonia nitrogen removal from aqueous solutions. *Bioresour. Technol.* **2019**, *292*, 121927. [[CrossRef](#)]
17. Yao, Y.; Gao, B.; Fang, J.; Zhang, M.; Chen, H.; Zhou, Y.; Creamer, A.E.; Sun, Y.; Yang, L. Characterization and environmental applications of clay–biochar composites. *Chem. Eng. J.* **2014**, *242*, 136–143. [[CrossRef](#)]
18. Ömeroğlu, A.; Erdoğan, Y.; Özcan, A.S. Modification of bentonite with a cationic surfactant: An adsorption study of textile dye Reactive Blue 19. *J. Hazard. Mater.* **2007**, *140*, 173–179. [[CrossRef](#)]
19. Zhang, D.; Zhang, Y.; Shen, F.; Wang, J.; Li, W.; Li, E.; Falandysz, J. Removal of cadmium and lead from heavy metals loaded PVA–SA immobilized *Lentinus edodes*. *Desalination Water Treat.* **2013**, *52*, 4792–4801. [[CrossRef](#)]
20. Chen, Y.; Yu, B.; Lin, J.; Naidu, R.; Chen, Z. Simultaneous adsorption and biodegradation (SAB) of diesel oil using immobilized *Acinetobacter venetianus* on porous material. *Chem. Eng. J.* **2016**, *289*, 463–470. [[CrossRef](#)]
21. Zhao, Y.-G.; Zheng, Y.; Tian, W.; Bai, J.; Feng, G.; Guo, L.; Gao, M. Enrichment and immobilization of sulfide removal microbiota applied for environmental biological remediation of aquaculture area. *Environ. Pollut.* **2016**, *214*, 307–313. [[CrossRef](#)] [[PubMed](#)]
22. Nie, H.; Nie, M.; Diwu, Z.; Wang, L.; Yan, H.; Lin, Y.; Zhang, B.; Wang, Y. Biological treatment of high salinity and low pH produced water in oilfield with immobilized cells of *P. aeruginosa* NY3 in a pilot-scale. *J. Hazard. Mater.* **2019**, *381*, 121232. [[CrossRef](#)] [[PubMed](#)]
23. Binnal, P.; Babu, P.N. Optimization of environmental factors affecting tertiary treatment of municipal wastewater by *Chlorella protothecoides* in a lab scale photobioreactor. *J. Water Process. Eng.* **2017**, *17*, 290–298. [[CrossRef](#)]
24. Ge, C.-H.; Dong, Y.; Li, H.; Li, Q.; Ni, S.-Q.; Gao, B.; Xu, S.; Qiao, Z.; Ding, S. Nitritation-anammox process—A realizable and satisfactory way to remove nitrogen from high saline wastewater. *Bioresour. Technol.* **2018**, *275*, 86–93. [[CrossRef](#)]
25. Gao, Y.; Wang, X.; Li, J.; Lee, C.T.; Ong, P.Y.; Zhang, Z.; Li, C. Effect of aquaculture salinity on nitrification and microbial community in moving bed bioreactors with immobilized microbial granules. *Bioresour. Technol.* **2020**, *297*, 122427. [[CrossRef](#)]
26. Li, L.; Wang, T.L.; Li, H.F.; Chen, J.Q.; Su, F.L. Effects of the Liao River Wetland on removal nitrogen. *J. Irrig. Drain.* **2012**, *31*, 137–139. [[CrossRef](#)]

**Disclaimer/Publisher’s Note:** The statements, opinions and data contained in all publications are solely those of the individual author(s) and contributor(s) and not of MDPI and/or the editor(s). MDPI and/or the editor(s) disclaim responsibility for any injury to people or property resulting from any ideas, methods, instructions or products referred to in the content.